Remote Sensing of Environment

www.elsevier.com/locate/sna

Mapping Complex Patterns of Erosion and Stability in Dry Mediterranean Ecosystems

Joachim Hill[*] *and Brigitta Schütt*[†]

Parametrizing soil reflectance spectra with variables related to specific shape characteristics of the spectral profile permits organic carbon concentrations in soils to be estimated on the basis of regionally validated regression models. An important feature of the approach is that it can not only be applied to continuous spectra but, without notable loss in accuracy, also to the spectral resolution of operational earth observation satellites such as the Landsat-TM or -ETM systems. Using this type of imagery, it can also be shown that soil organic matter is positively correlated to growth conditions for cereal crops in dryland agriculture. Strong correlations with qualitative erosion indicators that can be derived through spectral unmixing approaches demonstrate that soil organic matter is an important indicator for assessing land degradation processes in dry ecosystems from space. ©*Elsevier Science Inc., 2000*

INTRODUCTION

Although ecosystem processes with their implications for the future progress of land degradation have been intensely studied at numerous field sites in the Mediterranean region (e.g., Brandt and Thornes, 1996; Lacaze et al., 1996) it is difficult to extrapolate findings from field studies at patch scale to larger areas. Remote-sensing systems, and in particular Earth observation satellites, may significantly contribute to the solution of this problem by providing methodological pathways for scaling up the results of field measurements, and thereby supplying the spatial information needed for regional-scale analyses of the relationships between climate change and soil erosion or land degradation.

Whereas most remote-sensing studies have attempted to approach desertification and land degradation solely through mapping changes in vegetation cover and abundance, or land use in a general sense, this article deals with developing methods that also can derive state variables based on the reflectance characteristics of soils. Pickup and Chewings (1988) have already demonstrated that it is possible to link an erosion model with remote sensing for developing a valuable predictive tool, and Hill et al. (1995a) have shown how qualitative parameters indicative of soil conditions and degradation can be derived from multispectral images using spectral unmixing approaches. Here, we propose an approach for differentiating between more—or less—favorable areas on the basis of quantifying specific indicator substances in the soil. In particular, this article focuses on the organic carbon content in topsoils as an indicator for soil quality and soil erosion processes. In the context of landscape evolution, the spatial variability of soil organic matter concentrations might be understood as an indicator which emphasizes areas of accumulation and relative stability (sinks) in comparison to active erosion and transport cells (source areas).

THE STUDY SITE

This article presents results which are based on a field-mapping and sampling campaign carried out in parts of the Guadalentin watershed (Province of Almeria and Murcia) in southeastern Spain (Fig. 1). The study site belongs to the Cordillera Betica and its lithology is dominated by limestone and marls of Cretacious to Tertiary age. The region is in the most arid part of the Mediterranean basin. Average annual rainfall in the lowlands of the Guadalentin drainage basin is around 300 mm; only around the mountain tops might these values locally exceed 1000 mm per year (e.g., Geiger, 1970).

Particularly important for the aridity in SE Spain is the fact that most of the rainfall events yield little moisture (75% of all rainfalls are below 4 mm) which hardly exceeds infiltration capacity. High-intensity rainfalls which gener-

[*] Remote Sensing Department, University of Trier, Trier, Germany
[†] Department of Physical Geography, University of Trier, Trier, Germany

Address correspondence to J. Hill, Remote Sensing Dept., Univ. of Trier, 54286 Trier, Germany. E-mail: hillj@uni-trier.de
Received 27 September 1999; revised 10 May 2000.

REMOTE SENS. ENVIRON. 74:557–569 (2000)

655 Avenue of the Americas, New York, NY 10010

0034-4257/00/$–see front matter
PII S0034-4257(00)00146-2

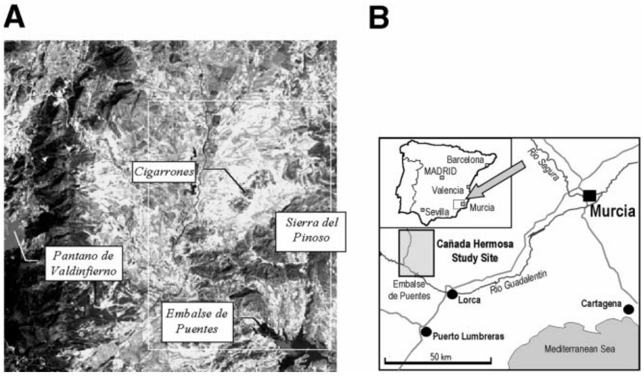

Figure 1. Location of the Cañada Hermosa study site in the Guadalentin Basin in SE Spain. a) Landsat TM image (25 July 1992, 10.06 h GMT, Path/Row 199-34, N37.5°/E358.3°, Sun elevation/azimuth: 57.2°/114.3°) of the limestone/marl areas south of Zarzilla de Ramos (Lorca); the study site is indicated by the rectangle. b) Index map showing the location of the study site (shaded rectangle).

ate substantial surface runoff occur rarely, but may reach enormous dimensions. In 1948, for example, the town of Puerto Lumbreras was largely devastated through torrential rains which delivered about 240 mm within several hr; in 1973 and 1997, the same town and many other locations in the region suffered again from severe flooding.

The Cañada Hermosa experimental site is located in the Subbetic zone and is dominated by large and softly rolling plains that dip in the main drainage directions. Mountainous terrain, such as the "Cigarrones" or the "Sierra del Pinoso" (Fig. 1), are adjacent to these plains. These carbonate ridges and hillslopes, now used exclusively for extensive grazing, are covered predominantly by grass tussocks (*Stipa tenacissima*) and coniferes (*Pinus halepensis*). At the base of the hillslopes colluvial zones lead into alluvial areas which are mainly used for rainfed agricultural production of grain crops. The soils are dominated by calcaric lithosols and regosols on sloping terrain, while calcaric fluvisols occur more abundantly in depressions or along the main river courses (Proyecto Lucdeme, 1988).

SOIL ORGANIC MATTER IN DRYLAND ECOSYSTEMS

Various important soil characteristics concerning the nutrient budget are determined through soil organic matter, such as the cation exchange capacity, soil acidity, the capacity of binding organic chemicals (pesticides, herbicides, fertiliser, etc.), the release and sequestration of N, P, and S during decomposition of soil organic matter, and nutrient availability for soil microorganisms (Volk and Loeppert, 1982). Besides the obvious impact of organic matter on chemical soil properties which directly affect the quality of the soil for agricultural use (Kononova, 1961), organic matter also influences the physical characteristics of a soil with regard to accelerated soil erosion processes, as, for example, hydraulic conductivity (percolation and retention of soil water), soil structure (type and size of soil aggregates), and soil color which influences albedo and soil temperature (Volk and Loeppert, 1982).

General models related to organic matter dynamics indicate that the physical characteristics of a soil reflect the balance between regenerative or degenerative processes of soil structure development. Stable macroaggregates (>250 μm) formed by inorganic compounds are, in general, held together by iron and aluminum oxides and occur predominantly in oxisols (Oades and Waters, 1991). Otherwise, stable macroaggregates are formed by soil organic matter such as fungal hyphae, fibrous roots, and polysaccharides. They rather occur under pasture or where organic residues have been added to the soil (Lynch and Bragg, 1985). The stability of macroaggregates increases with the amount of stable microaggregates (Tisdall and Oades, 1982; Tisdall, 1996). Since soil erodibility (i.e., the resistance to mechanical detachment and breakdown of soil aggregates, and the ability to accept rainfall as infiltration) is greatly influenced by the structural organization of the soil, it is obvious that highly calcareous silty Mediterranean soils become, in the absence of clay, highly dependent on organic matter (Imeson, 1995). Increased organic matter concentrations render these soils more favorable because of better aggregation, higher infiltration and water retention, and increased nutrient availability. Also, better infiltration of rainfall and the formation of macroaggregates are among the most important soil properties to increase their resistance to accelerated erosion.

Due to the low clay content of the soils in the study site, the production of stabilizing agents is primarily driven by causal loops involving organic matter production through biological activities (Dalal and Bridge, 1996). Since the agents of stabilization are consumed or degraded in the soil they need to be periodically replenished by biological activity (Fig. 2). If the balance between the amount of organic carbon being produced by plants is positive in relation to that being consumed by microflora, then the soil will produce either more or larger agglomerations of particles, thereby generating the positive feedbacks of increased aggregate stability, water, and nutrient availability required for sustained plant growth and reduced erodibility (Imeson et al., 1996).

RELATIONSHIPS BETWEEN SPECTRAL REFLECTANCE AND SOIL ORGANIC CARBON CONCENTRATIONS

Organic matter content is also a soil property that significantly influences the bidirectional reflectance characteristics of a soil substrate. As a result of many laboratory experiments on soil reflectance patterns (e.g., Condit, 1972, Stoner and Baumgardner, 1981; Baumgardner et al., 1985), it is understood that not only the general brightness (albedo) of soil spectra but in particular the shape of the spectral continuum between 0.35 μm and 1.4 μm is largely

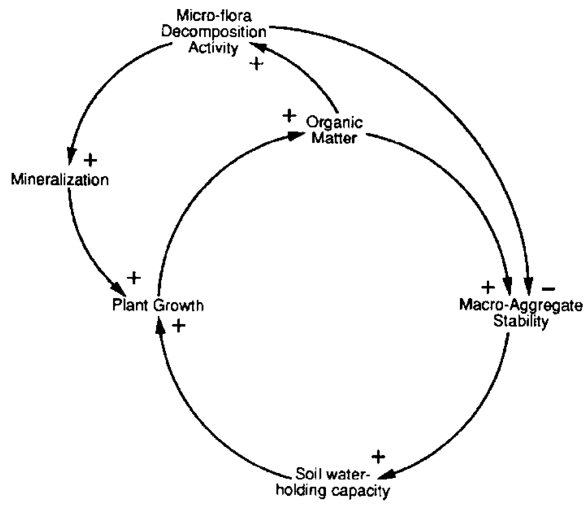

Figure 2. Causal-loop diagram illustrating the feedback relationships in aggregate growth from primary particles (Imeson et al., 1996).

determined by organic carbon. In case of low organic matter concentrations the reflectance curve of bare soils tends to be convex (Fig. 3, curve B). Organic carbon absorbs energy across the whole wavelength range up to 1.4 μm. It decreases overall albedo, but mainly causes the shape of the soil spectrum to become more concave from the visible to the short-wave infrared region (Fig. 3, curve A).

Although the general relationship between organic matter and soil brightness and color has long been recognized, quantifying this has been difficult because soil reflectance is influenced by additional properties such as soil moisture, the content of iron, or mafic minerals. Soil texture controls whether relationships between soil organic matter and soil color are linear (in silty and loamy soils) or curvilinear (sandy-textured soils). Summarizing the results of a review paper by Schulze et al. (1993), relationships between soil organic matter and reflectance properties can be developed within and even among soil landscapes if soil textures are not too variable, but may become unpredictable if soil texture varies too widely.

Figure 3. Characteristic soil bidirectional reflectance spectra (Baumgardner et al., 1985). Curve A: developed, fine textured soils with high (>2%) organic matter content; B: undeveloped soils with low (<2%) organic matter and low (<1%) iron oxide content; C: developed soil with low (<2%) organic matter and medium (1–4%) iron oxide content; D: moderately coarse textured soils with high (>2%) organic matter content and low (<1%) iron oxide content; E: fine textured soils with high (>4%) iron oxide content.

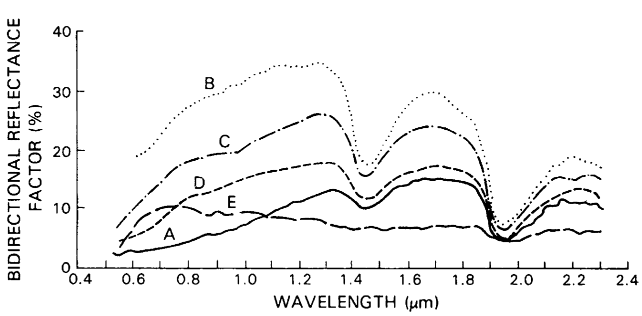

Most of the early studies identified relations between organic carbon content and spectral variables based on the reflectance in the visible range of the solar spectrum (Shields et al., 1968; Al-Abbas and Baumgardner, 1972; Page, 1974). In continuing this work, major efforts concentrated on correlating specific spectral bands with soil organic matter. Leger et al. (1979), for example, used the area ratio between reflected and absorbed radiation in specific wavelength intervals of the visible spectrum as variables to determine the organic matter content through multiple regression. Similar approaches extended the spectral variables used into the near-infrared and attempted to include additional variables describing more closely the shape of the spectral profile (Krishnan et al., 1980). More recently, Ben-Dor and Banin (1994) used the full reflective spectrum to predict soil organic matter and other mineralogical and chemical soil properties based on multivariate statistics. The same approach was then applied to a reduced number of spectral bandpasses as provided by the Landsat Thematic Mapper (Ben-Dor and Banin, 1996).

Even though some of these studies proved to be successful under laboratory conditions it should be emphasized that they were rarely, or not at all, applied to the interpretation of real multispectral imagery. This is mainly due to the following issues:

1. The relationship as such is weak and statistically not convincing.
2. The relationship can not be transferred to the limited band set of an operational sensor system.
3. It is not evident for which reason specific spectral bands have been selected to derive the relationship.
4. The application of the relationship to real images fails because of insufficient calibration of the image data (i.e., compensation of atmospheric effects).

To overcome these shortcomings, it will be necessary to combine a validated model for predicting soil organic carbon from spectral reflectance with specific image-processing techniques required to compensate undesired image characteristics.

FIELD SAMPLING AND LABORATORY ANALYSIS

Along several transects in the Cañada Hermosa site (Fig. 4) a total of 92 soil samples were taken for analysis in the laboratory. For each sampling location specific variables, such as stone cover, Munsell soil color, slope angle, plan curvature, as well as convexity and concavity of the slope segment, were recorded. Reflectances were measured in

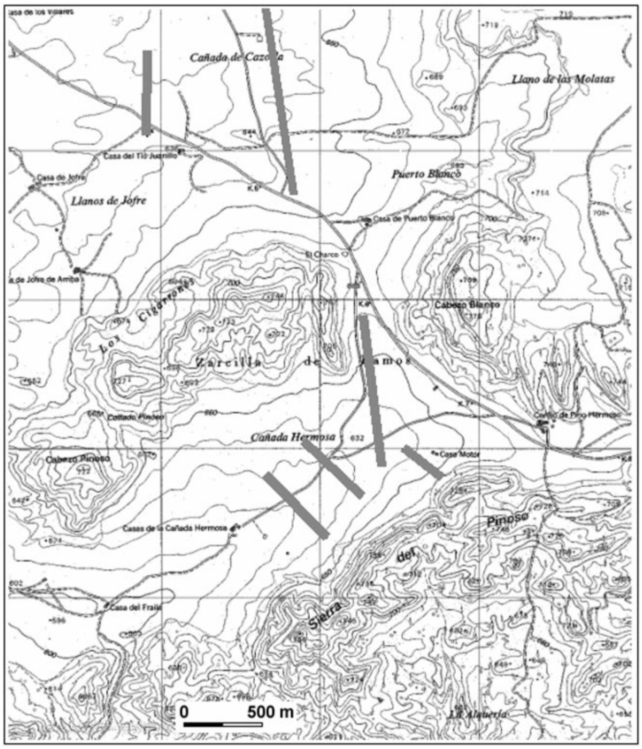

Figure 4. Sampling transects in the Cañada Hermosa study site.

the field and in the laboratory with a high-spectral-resolution ASD FieldSpec II Spectroradiometer, covering the spectral range between 0.35 μm and 2.5 μm. The spectral recordings taken in the field were exclusively used for validating the results of the radiometric (i.e., atmospheric) correction of the satellite scenes in reference to largely invariant surfaces.

The soil chemical analysis of the samples included the detection of organic and inorganic carbon using a high-frequency induction furnace. The analysis involved two phases, one between 200°C and 550°C for organic carbon and the other between 550°C and 1050°C for inorganic carbon. While temperature is increased at a rate of 200°C/min, the CO_2 flow is continuously detected by an infrared cell. The accuracy of the measurements is specified to 1.5% of the detected amount, with a detection limit of 0.02% (all percentages are weight %, unless otherwise indicated). It was found that the organic carbon content in the studied soils is highly variable (0.08–1.67%, n=92), but does not exceed 2%.

The mineral composition of the soil samples was analyzed by X-ray powder diffraction (2–70° 2Θ Cuk$_{\alpha}$). Based on the intensity of the diffraction pattern and referring the intensity relations of the dominant X-ray diffraction peaks of calcite and dolomite to the data of inorganic carbon content, mineral contents for calcite, dolomite, and quartz were quantified (Behbehani, 1987). An important feature of the soils is their very high carbonate content (predominantly calcite) which amounts to 74.6 [% $CaCO_3$] (std. dev.=5.13, n=92). Average quartz content totals 5.8%, and the average content of clay minerals in the soils does not exceed 6.7%; silicates are thus of minor significance for the mineralogical composition of the soils. Especially the low content of clay or clay minerals is important because low-clay soils are sensitive to the loss of organic matter, which largely determines their resistance to erosion.

Grain-size distribution in the soil samples was analyzed for a subset of 29 samples from two representative transects by separating firstly the sand fraction (>63 μm) by wet sieving (H_2O). The size fraction <63 μm was further differentiated by a GALAI CIS-1 particle analyzer which detects particle size using a focused, fast-rotating 600 mW He-Ne laser beam. For identifying the size of microaggregates, the samples were measured dispersed in H_2O without supplementary preparation. In continuation of the analysis, all samples were treated for 20 min by ultrasound to destroy the microaggregates. Repeating the particle-size analysis now reveals the grain-size distribution of nonaggregated particles. The grain size distribution of the Cañada Hermosa soils indicates a predominance of silty to sandy components.

For identifying relationships between selected chemical soil parameters and landscape elements related predominantly to soil erosion and transport (source areas) or deposition (sinks) statistical averages and SDs of the different soil constituents were tested against various morphometric variables, such as slope profile and plan curvature. These data indicate that significantly higher contents (α<0.001) of organic carbon (C_{org}) are found in areas with converging water flow (plan-concave slope elements) than in areas with diverging flow directions (i.e., plan-convex terrain units, corresponding to active erosion zones). For the same locations the concentrations of inorganic carbon (C_{inorg}) and calcite, which is primarily derived from the parent rock, are complementary to the organic carbon contents (α<0.001). This again supports the main hypothesis that areas of active erosion (sources) have significantly higher calcite contents than areas of deposition (sinks).

SPECTRAL MODELING AND SPATIAL MAPPING OF SOIL ORGANIC CARBON CONCENTRATIONS IN THE CAÑADA HERMOSA SITE

For the spectral measurements in the laboratory the optical head of the ASD FieldSpecII was mounted on a tripod with a viewing angle of 0°. The distance between optical head and sample or reference panel (Spectralon) was 30 cm. Both the soil samples and the reference panel were illuminated with a 1000-W quartz-halogen lamp mounted at a distance of approximately 50 cm and an illumination angle of 30°. Absolute bidirectional reflectance spectra were obtained by multiplying the raw reflectance spectra by the certified reflectivity of the Spectralon standard.

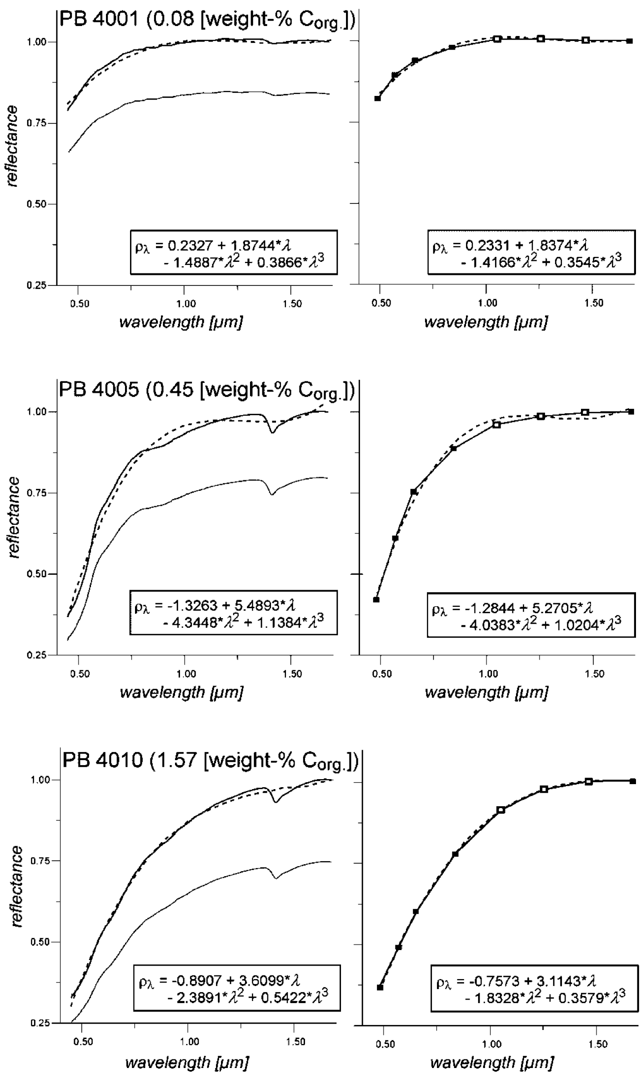

Figure 5. Original and peak-normalized spectral reflectance of continuous (left) and TM-resolved spectra (right) in comparison to the corresponding third-order polynomials [0.45–1.676 μm] for selected samples from the Cañada Hermosa site. Soil organic carbon concentrations range from 0.08 to 1.57 [wt % C_{org}]. The different line signatures indicate: ——— original spectra, ▬▬▬ peak-normalized spectra, ■ ■ ■ polynomial fit. The □ - symbols indicate supplementary anchor points in TM resolution.

Optimized Spectral Parameters for Modeling Soil Organic Carbon

As it is well understood that surface roughness effects due to cultivation, soil crusting, and terrain illumination influence the absolute reflectance of otherwise identical soils, measurements have been peak-normalized. This normalization was done with reference to the wavelength range between 1.5 μm and 1.6 μm, where most soils and rocks reach their maximum reflectance. Specifically, the wavelength of 1.676 μm was selected because it is in the bandpass of Landsat-TM Channel 5 and allows to process also TM-resolved spectra (Fig. 5).

Since the specific influence of soil organic matter (SOM) on spectral reflectance is not expressed in narrow absorption bands, as is, for example, the case for iron oxides or carbonates (Hunt and Salisbury, 1971; Hunt, 1977; Clark et al., 1990), but determines the overall shape of the reflectance between 0.35 μm and 1.4 μm (Fig. 5), we propose parametrizing the shape of the reflectance continuum in this wavelength range through the coefficients of a third-order polynomial [Eq. (1)]

$$\rho_\lambda = b_0 + b_1 \cdot \lambda + b_2 \cdot \lambda^2 + b_3 \cdot \lambda^3 \tag{1}$$

fitted to the spectra which can usually approximate the reflectance continuum of soils and rocks quite accurately. Whereas the constant term (b_0) of the polynomial relates to the intersection of the curve with the ordinate, coefficients $b_1 - b_3$ describe slope and curvature of the function. It results from a detailed statistical analysis of the spectral data involved in this study that coefficients b_1 and b_3 were the most important variables to characterize the reflectance continuum as a function of the organic carbon concentration. Then, coefficients b_1 and b_3 of the resulting equations were introduced as independent variables into a multiple linear regression analysis to determine the corresponding soil organic matter concentration[1]. Accounting for nonlinearities in the relationship, the logarithm of soil organic matter concentration (ln C_{org} [wt %]) can be modeled from the continuous spectra with

Model 1.0

$$\ln C_{org}\ (\text{wt } \%) = -1.885 + 1.591 \cdot b_1 - 6.552 \cdot b_3,$$

$$n = 91, \quad \text{multiple } r = 0.88734, \quad \text{adj } r^2 = 0.78501. \tag{2}$$

The significance of the independent variables b_1 and b_3 in *Model 1.0* is each $\alpha < 0.001$. Cross-validation of *Model 1.0* indicates a high quality ($n=91$, multiple $r=0.87762$, adj $r^2=0.76766$) of the relationship. The comparison of measured and predicted organic carbon concentrations (ln $C_{org.}$ [wt %]) exhibits an offset close to 0, and the slope of the linear regression between measured and predicted concentrations is close to 1 (Fig. 6).

The application of this approach to reflectance measurements in the spectral resolution of the Landsat Thematic Mapper requires some modification. Again, in a first step the TM-resolved spectra are peak-normalized to the reflectance at TM Channel 5 (i.e., 1.676 μm). However, in order to fit a third-order polynomial to the peak-normalized reflectance in TM Channels 1–5, additional spectral reflectance values at $\lambda = 1.049$ μm, 1.258 μm, and 1.467 μm derived from a cubic spline interpolation (stretching factor=0.9) of the available TM bands were used to compute the polynomial coefficients (Fig. 5). This leads to Eq. (3):

[1] Variable b_0 was not significant, b_2 excluded with regard to colinearity analysis.

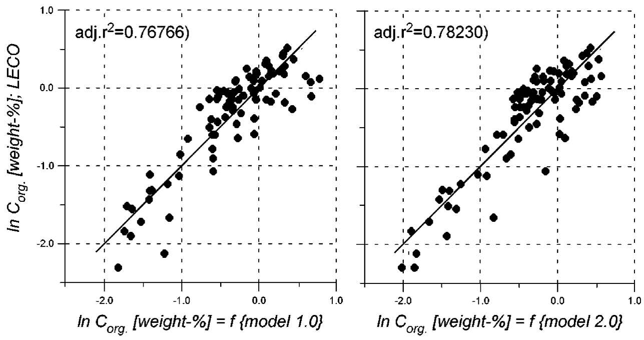

Figure 6. Scatter-plots of the cross validation between modeled and laboratory-measured soil organic carbon concentrations (ln C_{org} [wt %]) as derived from continuous (Model 1.0, left), and TM-resolved spectra (Model 2.0, right).

Model 2.0

$$\ln C_{org}\ (\text{wt }\%) = -2.519 + 1.808 \cdot b_1 - 7.768 \cdot b_3,$$

$$n=91, \qquad \text{multiple } r=0.89239, \qquad \text{adj } r^2=0.79410, \tag{3}$$

where the significance of the independent variables b_1 and b_3 is each $\alpha<0.001$. Cross-validation of *Model 2.0* also shows a high quality ($n=91$, multiple $r=0.88583$, adj $r^2=0.78230$) and, as for *Model 1.0*, comparison of measured and predicted organic carbon contents (ln $C_{org.}$ [wt %]) exhibits an offset close to 0 with a regression slope close to 1 (Fig. 6).

In order to validate the efficiency of the proposed approach to predict soil organic matter from spectral reflectance the results have been compared to some of the methods mentioned in the available literature (Table 1). In each case, the analysis was based on all available samples. It is seen that the parametrization of the spectral continuum through selected coefficients of a third-order polynomial fit to continuous reflectance measurements provides better results than the alternative approaches. More important, however, is the fact that the positive results are confirmed when reflectance spectra with the reduced spectral resolution of the Landsat Thematic Mapper are used.

Mapping Soil Organic Carbon Based on Earth Observation Satellite Data

Given the many studies relating spectral variables to the concentration of specific substances in soils, it is surprising that hardly any of the proposed relationships has been applied to map soil differences on real images. As the approach discussed in this article is applicable to high-resolution spectra as well as to the sequence of discrete bandpasses provided by the Landsat Thematic Mapper, a case study can be presented which outlines the pathway to produce spatially differentiated maps of soil organic matter.

Geometric and Radiometric Preprocessing of Satellite Data

This case study is based on three images from the Guadalentin study site obtained by the Landsat Thematic Mapper system (WRS 199/34) on 1 July 1989, 20 April 1992, and 25 July 1992. Although it is feasible to use single images from well-chosen phenological phases (in our study region

Table 1. Comparison of Different Methodological Approaches Predicting Soil Organic Matter by Spectral Reflectance Features, Generated by 100% of Total Data ($n=91$)

	Independent Variables	*Dependent Variable (wt %)*	*Multiple* r	*adj* r²	*Regression*	*Authors*
Model 1.0	Coefficients b_1, b_3 of a third order polynomial curve fit to peak-normalized continuous reflectance [0.45; 1.676] μm	ln C_{org}	0.88734	0.78501	Multiple, linear	This work
Model 1.1	Linear regression of non-std. average refl. at [0.45; 0.70] μm (panchromatic)	C_{org}	0.72366	0.51839	Linear	Page (1974)
Model 1.2	Exponential regression non-std. average reflectance at [0.45; 0.70] μm (panchrom.)	C_{org}	0.85580	0.72942	Exponential	Page (1974)
Model 1.3	Linear regression non-std. average reflectance [0.60; 0.66] μm	C_{org}	0.68982	0.47003	Linear	Page (1974)
Model 2.0	Coefficients b_1, b_3 of a third order polynomial fit to normalized TM 1–5 reflectance	ln C_{org}	0.89239	0.79410	Multiple, linear	This work
Model 2.1	Multiple regression of non-std. reflectance at TM Channels 1, 3, and 4	C_{org}	0.83569	0.69502	Multiple, linear	Ben-Dor and Banin (1996)
Model 2.2	Multiple regression of std. reflectance at TM Channels 1, 3, and 4	C_{org}	0.83320	0.69083	Multiple, linear	As above, standardized

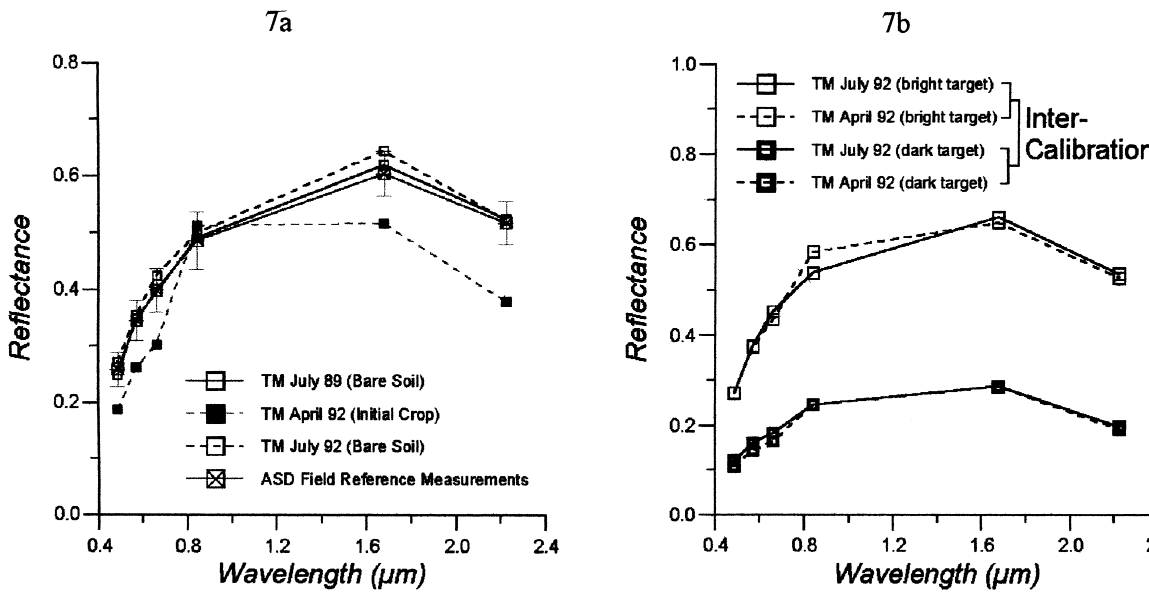

Figure 7. Landsat-TM average reflectance of the calibration target (7/89 and 7/92) in comparison to mean and ±1 S.D. of the corresponding field measurements (left). The 4/92 scene (sparse vegetation cover within the primary reference area) has been intercalibrated to the image from 7/92 based on bright and dark reference targets with negligible (i.e., ≤5%) vegetation cover (right).

preferably late spring) the multitemporal approach provides specific advantages because the combination of mapping results from several dates may efficiently compensate local artifacts due to residual dry vegetation (crop residue) in the farmed areas. All images have been coregistered and georeferenced to the UTM-projected topographic maps of the study region at scale 1:25,000 (Mapa Topográfico Nacional de España, sheets 953-I, 952-II, 931-IV, 932-III) with subpixel accuracy (RMS errors range from 0.35 to 0.7 pixels, i.e., 10.5–21 m).

Since a basic prerequisite of our approach is that the spectral information be provided on the level of bidirectional reflectance, all images needed to be corrected for atmospheric effects. This was achieved by applying a radiative transfer code (Hill and Sturm, 1991; Hill, 1993), which is largely based on analytical functions provided by Tanré et al. (1990). More recently, this modified 5S code has been further improved by adding a formalism to account for terrain-induced illumination effects (Hill et al., 1995b). Thematic Mapper calibration changes over time have been accounted for by using data from Thome et al. (1993; 1997) and our own assessments published in Lacaze et al. (1996). Using standard values for atmospheric water-vapor absorption (which affects TM data mainly in the near-infrared and short-wave infrared bands) the only important unknown to be determined for each image was the aerosol optical depth. Since no suitable dark objects are available in the study region which may permit the estimation of this parameter from the scene itself (e.g., Royer et al., 1988; Hill, 1993), standard aerosol optical depth values have been iteratively adjusted until they reproduced field-recorded reference spectra from a bare soil calibration surface with acceptable accuracy (Fig. 7). By incorporating commercially available digital elevation data derived from SPOT panchromatic images (©ISTAR), it was possible to obtain illumination-corrected reflectance images for all three dates.

Compensation of Vegetation-Related Effects on Soil Reflectance

A common problem in the analysis of soil spectra in real images is the partial coverage by green or dry vegetation. Particularly in agricultural areas, the proportion of dry vegetation (i.e., crop residue) mainly depends on the date of image acquisition. While no soil-related spectral information can be detected over fully plant-covered surfaces (which must be recovered from other images on which the soil surface is exposed), it is possible to use specific image-processing options for retrieving soil spectral characteristics from only partially plant-covered areas. An efficient approach for achieving this objective is based on spectral decomposition techniques as used in spectral mixture analysis (SMA) (e.g., Adams et al., 1993; Hill et al., 1995a; Nielsen, 1998).

Full spectral unmixing builds on the premise that the overall reflectance within a sensor's instantaneous field-of-view is due to additive mixtures of the reflectance properties of the individual surface components present therein. The spectral reflectance is thus modeled as a linear combination of pure component (i.e., endmember[2]) spectra in Eq. (4):

[2] Endmembers are pure pre-determined classes with 100 % abundance of one element and with no mixtures.

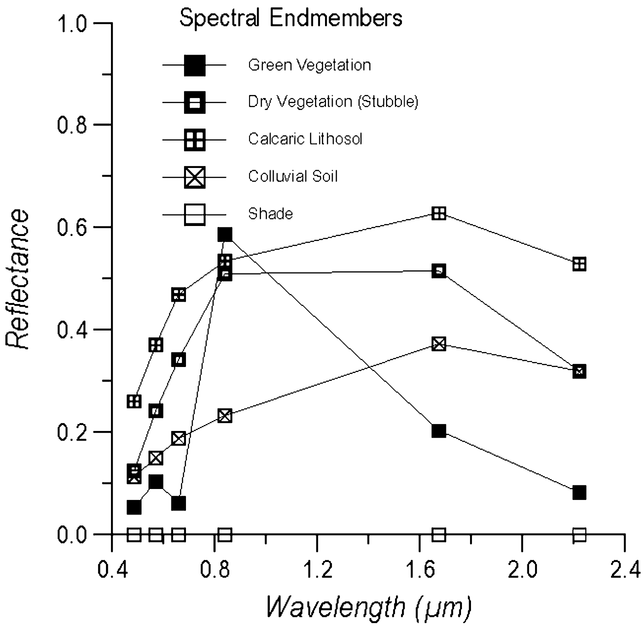

Figure 8. Spectral endmembers used for the forward/inverse modeling of spectral mixtures of the Landsat TM images included in this study.

$$R_i=\sum_{j=1}^{n}F_j\cdot RE_{ij}+\varepsilon_i \qquad \text{and} \qquad \sum_{j=1}^{n}F_j=1, \tag{4}$$

where R_i is the reflectance of the mixed spectrum in band i, RE_{ij} is reflectance of the endmember spectrum j in band I, F_j denotes the estimated proportion of endmember j, and ε_i the residual error in band i (i.e., band residual), which might be due to improperly chosen or an insufficient number of endmembers. When imposing the constraint that the abundance estimates sum to 1, a unique solution is possible as long as the number of spectral components does not exceed the number of bands plus 1. Negative abundance estimates or values exceeding 100% have been accepted within limited bounds, that is, $-0.1\leq F_j\leq 1.1$, larger deviations were discarded from further analysis.

Already Adams et al. (1989) have proposed that the spectral-mixing paradigm can be used to exclude the spectral contribution of vegetation ("spectral defoliation"). This is achieved by rescaling the remaining abundance estimates to 100% after discarding the proportion of the vegetation endmember. Multiplying the resulting abundance vector with an equivalently reduced endmember matrix (i.e., where the vegetation endmember has been removed) yields a model of the original image for which, provided that the mixing model has only generated negligible RMS errors and band residuals, the spectral characteristics of photosynthetic vegetation are substantially reduced in comparison to the background signal. We have used this approach to compensate the influence of a partial coverage by wheat and barley in the TM image from spring 1992. The used endmember combination is shown in Figure 8, and it needs to be pointed out that the unmixing-based restoration of soil spectral information was only applied for surfaces with a vegetation abundance estimate below 50%. Areas which do not comply to this restriction (i.e., $F_{veg}>0.5$), or which exhibit prohibitively large modeling errors (in terms of

Figure 9. Color composites (RGB=bands 4-5-3) of the original Landsat-TM reflectance image from April 1992 (left) and its "defoliated" version where areas with $F_{veg}>0.5$ have been masked in white (right). The imaged area is outlined in Figure 1.

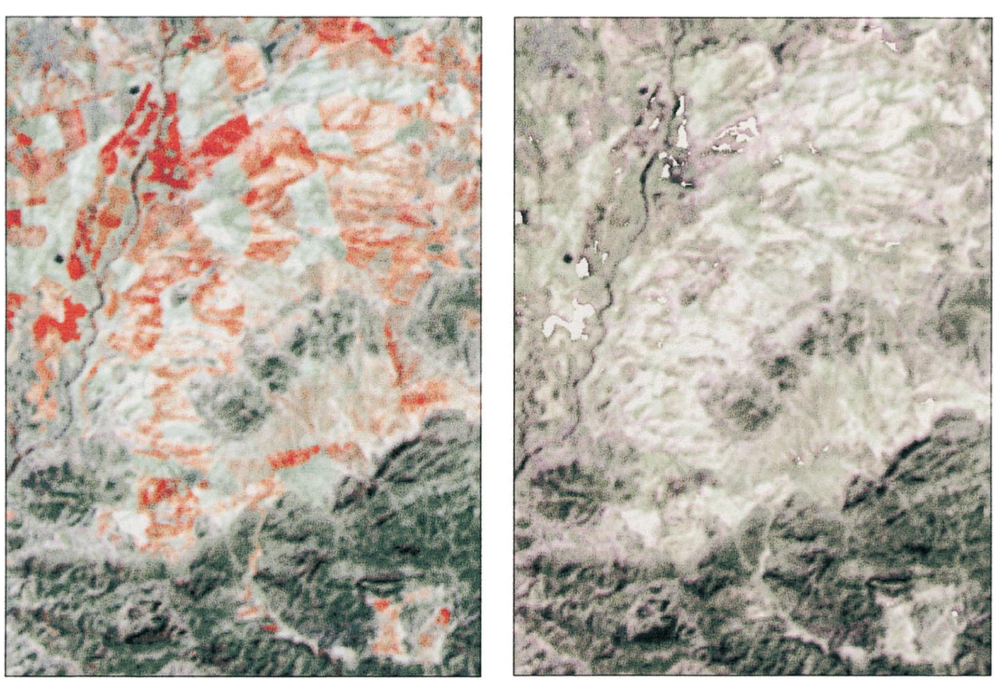

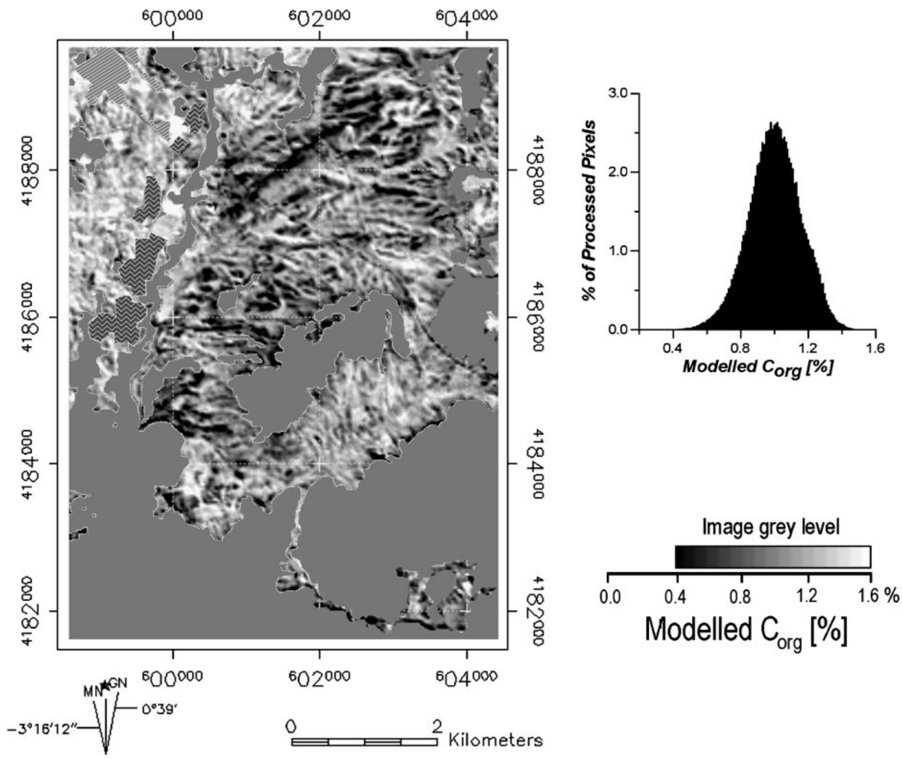

Figure 10. Average soil organic carbon concentrations (C_{org}) derived from applying Model 2.0 to three Landsat Thematic Mapper images (7/89, 4/92, and 7/92) of the Cañada Hermosa Study Site. The histogram upper right shows the distribution of C_{org} values in the imaged area; the gray scale relates image gray tones to C_{org} values.

RMSE and band residuals) were removed from the modeled image (Fig. 9)

Satellite Mapping of Organic Carbon in Soils

Each of the preprocessed images has been analyzed using the laboratory-calibrated model (Model 2.0) as described and discussed earlier in this article. Although this approach involves substantial scale transitions, the resulting histograms of the modeled C_{org}-values cover a realistic range; only very low and high values seem underrepresented (Fig. 10). This might be explained as an effect caused by the spatial resolution of the Thematic Mapper system: Surfaces with extremely low organic carbon contents preferentially occur near rock outcrops and have limited spatial extent. Similarly, organic matter contents close to, or above 2%, are only found below perennial plants or in small accumulation areas. It is evident that such surface elements are not spatially resolved by the TM system with its instantaneous field of view of 30×30 m^2.

To minimize potential estimation errors due to particular land cover properties at the time of image acquisition (e.g., the presence of crop residue, weeds, soil surface effects due to ploughing, and other types of soil cultivation, etc.), the final map of soil organic carbon concentrations has been produced by averaging the modeling results obtained from the three individual scenes (Fig. 10). Since the relationship between soil organic carbon and reflectance properties is only specified and validated for agricultural soils, all areas with seminatural permanent vegetation have been excluded from the modeled area. Also, urbanized zones (Zarzilla de Ramos) and irrigated areas with dense plant cover in at least two of the TM scenes have not been mapped.

Thus, a continuous and spatially differentiated map of soil organic carbon concentrations has been obtained which displays continuous geomorphic features from which spatial structures related to agricultural land use have been removed (e.g., Fig. 10). A drainage pattern is obvious that originates from more elevated rangelands and, following local flow directions, finally connects to the Rio Turilla which crosses the western part of the image from north to south. This pattern, emphasized by variable organic carbon concentrations in the topsoil, is understood as an erosion cell mosaic in the sense of Pickup and Chewings (1988). Along elevated ridges and on erosive slope segments (source areas) these concentrations are generally low, while higher amounts of soil organic carbon preferably occur in transport and accumulation zones (sediments sinks).

RESULT ANALYSIS AND DISCUSSION

In the context of assessing land degradation in dryland ecosystems, most remote-sensing studies have focused on vegetation cover as an indicator of land suitability or degradation. Only few studies, for example, Pickup and Chewings (1988), Escadafal et al. (1994), and Hill et al. (1995a), have been able to use also parameters indicative of soil conditions and hence to apply concepts taken from pedology and geomorphology to obtain qualitative, but still reliable indications for soil degradation or erosion processes.

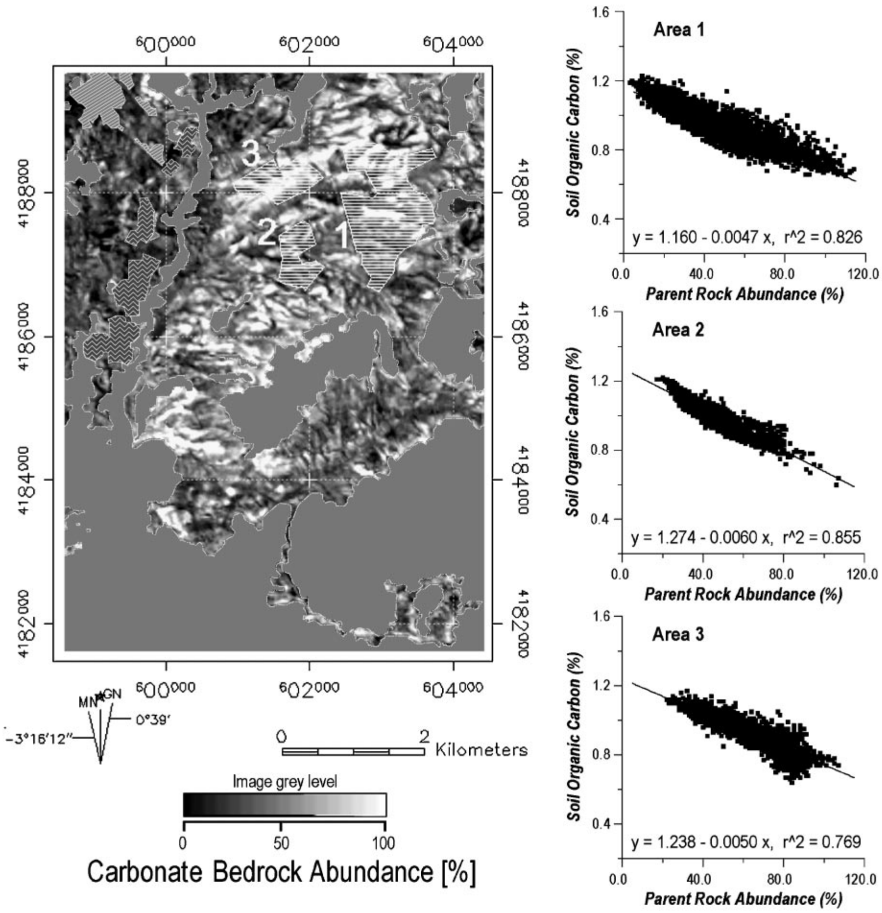

Figure 11. SMA-derived map of qualitative soil erosion indicators, displaying the average proportion (in %) of carbonate parent material exposed at the surface (i.e., a maximum value composite derived from three Landsat images). The scatter plots, obtained from selected reference areas in the farmed areas, document the strong correlation which exists between SMA-derived qualitative erosion indicators and the quantified soil organic carbon concentrations derived from the Landsat TM images.

Pickup and Chewings (1988) in Australia conceptualized an approach whereby the landscape is divided into production zones with net soil loss, transfer zones with intermittent erosion and deposition, and sink areas where accumulation occurs. Several production zones may share one sink; vegetation growth in the sink reinforces alluviation and enhances its stability with respect to erosion. Hill et al. (1995a) were able to map areas affected from soil degradation and erosion under subhumid conditions in Mediterranean France based on spectral mixture analysis. Their approach was based on estimating the amounts of rock fragments and soil particles on the surface. Since, within a specific context, soil erosion leads to an increase of the proportion of bedrock components in source areas and the accumulation of soil material in sediment sinks, the relative proportion of parent material at the soil surface could be interpreted as an indicator of degradation. This corresponds to defining the erosional state of soils as a function of the mixing ratio between developed soil substrates and parent material components which, of course, need to be spectrally distinct from each other (Hill et al., 1995a).

Accordingly, a qualitative indicator map of soils with truncated soil profiles (i.e., affected by erosion) was derived through analyzing the spectral mixtures in the Landsat TM images covering the Cañada Hermosa site. Here, a field-measured reflectance spectrum of a typical carbonate lithosol (see Fig. 8) has been chosen to represent the material which is usually exposed at outcrops of the parent material. In the case that the proportional abundance of this material within a pixel becomes dominant, it was concluded that the site is affected by severe soil erosion. The individual lithosol fraction images derived for the three scenes have been combined into a single image, following a classical maximum-value-compositing technique. Interestingly enough, it can be shown that the proportional abundance of poorly weathered bedrock material in the topsoil is inversely correlated with the soil organic carbon estimates discussed before (Fig. 11). It is thereby suggested that organic carbon is a tracer substance which highlights areas of accumulation and relative stability (sinks) where soil conditions are favorable because of higher infiltration and water retention capacity, better aggregation, and increased nutrient availability. One can thus conclude that the SMA-derived qualitative indicators are corroborated in comparison to the quantitative estimates of soil organic carbon which are suited to provide a more systematic basis for defining soil degradation maps, that is, by defining appropriate threshold levels in terms of C_{org} concentrations.

The relatively high concentration of soil organic carbon in the sediment sinks is probably not exclusively caused

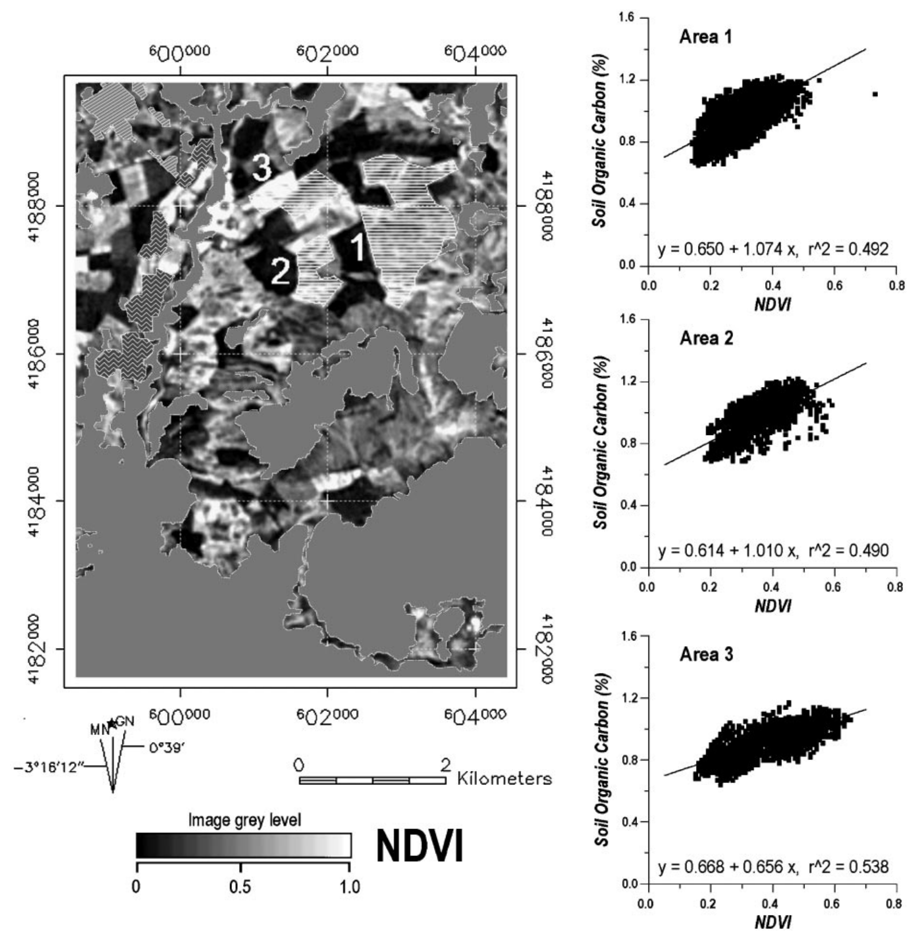

Figure 12. Normalized difference vegetation index (NDVI) computed for the Landsat Image from April 1992 (left). The scatter plots, obtained from selected reference areas within the farmed areas, clearly emphasize the positive correlation between the vegetative growth of the cereal crop and the soil organic carbon concentrations derived from the Landsat TM images.

by deposition processes during respectively after rainfall and runoff events but also results from the lateral removal of topsoil by ploughing and the increased SOM *in situ* production, driven by the positive feedback organic matter exerts on soil structure, water infiltration and nutrient availability, and, therefore, plant growth and plant residue available for further decomposition. It is quite remarkable that also the positive impact of increased organic matter concentrations on resource availability in the soils can be verified based on the Landsat images used in this study. The image which is best suited for such a validation is the TM scene from April 1992 because it captures the agricultural areas during a phase of spatially variable plant growth.

It is common sense that, under low rainfall conditions, plant density and growth rate of wheat and barley are significantly correlated to soil water available in the root zone. Since we hypothesized that soil organic matter has a positive influence on soil structure which, in turn, favors infiltration and water availability, we would expect that soil organic matter and plant density in agricultural areas are positively correlated. We thus compared a simple indicator for photosynthetic vegetation within selected cereal cropping areas in the Landsat image with their corresponding image-derived organic carbon concentrations (Fig. 12). It can be shown that this positive correlation, albeit not very strong, does in fact exist.

Notwithstanding the scale transitions implied, this underlines that, in case a robust prediction model for selected soil properties is coupled with specifically suited image processing techniques, Landsat images can provide quantitative and spatially differentiated information about soil resources which may be used for drafting and implementing development schemes for a sustainable use of marginal lands.

CONCLUSIONS

A specific approach to parametrize reflectance spectra of soil surfaces has been developed which permits the estimation of soil organic carbon concentrations in topsoil substrates from dry ecosystems with acceptable accuracy. It was further demonstrated that the model can be applied to multispectral images acquired by operational earth observation satellites with adequate spectral resolution (e.g., Landsat-TM), or corresponding airborne imaging systems. Within the spatial resolution capacity of the sensor system, the approach permits the production of spatially differentiated maps of soil organic carbon. It is expected that the usefulness of this approach may further increase with the availability of high quality imaging spectrometers becoming more frequent.

What needs to be taken into consideration, however, is the fact that the statistical model to predict soil organic carbon from spectral reflectance data is so far limited to soils on carbonate bedrock. Considering the dependence of model type and variables on specific soil parameters it is evident that such estimators need to be re-calibrated for individual "soilscapes."

In relation to the positive feedback loops which are driven by organic matter in soils, information about the concentration of soil organic carbon provides an important indicator for soil quality, that is, one of the important variables to be considered in land-use planning and development strategies, but also in establishing precision farming systems. A thorough assessment of available resources, the implementation of adequate management strategies and efficient approaches to monitor the state of the environment are the core elements on which to build efficient strategies to mitigate land degradation and desertification risks. It is also believed that further integration of remote sensing and GIS-based modeling approaches will substantially support each of these issues.

This work was financially supported through the ERMES-II (Erosional Response of Mediterranean Ecosystems) projects (ENV4-CT95-0181) funded by the European Commission, Directorate General XII for Science, Research and Development, in the frame of the Environment and Climate Program (1994-1998). The assistance of A. Imeson and L. H. Cammeraat (both University of Amsterdam), and S. Sommer (European Commission, Space Applications Institute, Joint Research Centre) during field work in the Canada Hermosa was highly appreciated. The Space Applications Institute of the Joint Research Centre also provided part of the satellite data used in the study. This support is gratefully acknowledged.

REFERENCES

Adams, J. B., Smith, M. O., and Gillespie, A. R. (1989), Simple models for complex natural surfaces: a strategy for the hyperspectral era of remote sensing. In *Proc. of the IGARSS '89 Symposium*, 10–14 July, IEEE, Vancouver, Canada, pp. 16–21.

Adams, J. B., Smith, M. O., and Gillespie, A. R. (1993), Imaging spectroscopy: interpretation based on spectral mixture analysis. In *Topics in Remote Sensing IV: Remote Geochemical Analysis* (C. M. Pieters and P. A. J. Englert, Eds.), Cambridge University Press, Cambridge, pp. 145–166.

Al-Abbas, A. H., and Baumgardner, M. F. (1972), Relating organic matter and clay content to the multispectral radiance of soils. *Soil Sci.* 114:477–485.

Baumgardner, M. F., Silva, L. F., Biehl, L. L, and Stoner, E. (1985), Reflectance properties of soils. *Adv. Agron.* 38:1–44.

Behbehani, A.-R. (1987), Sedimentations- und Klimageschichte des Spät- und Postglazials im Bereich der nördlichen Kalkalpen (Salzkammergutseen, Österreich). *Göttinger Arbeiten zur Geologie und Paläontologie*, 34. Geolog. Lust.: Göttiugen, 132 pp.

Ben-Dor, E., and Banin, A. (1994), Visible and near-infrared (0.4–1.1 μm) analysis of arid and semiarid soils. *Remote Sens. Environ.* 48:261–274.

Ben-Dor, E., and Banin, A. (1996), Evaluation of several soil properties using convolved TM spectra. In *Monitoring Soils in the Environment with Remote Sensing and GIS* (R. Escadafal, M. M. Mulders, and L. Thiombiano, Eds.), ORSTOM Editions, Paris, pp. 135–149.

Brandt, C. J. and Thornes, J. B. (1996), *Mediterranean Desertification and Land Use*, Wiley, Chichester.

Clark, R. N., King, T. V. V., Kleijwa, M., Swayze, G. A., and Vergo, N. (1990), High spectral resolution reflectance spectroscopy of minerals. *J. Geophys. Res.* 95:12,653–12,680.

Condit, H. R. (1972), Applications of characteristics vector analysis to the spectral energy distribution of daylight and the spectral reflectance of American soils. *Appl. Opt.* 11:74–86.

Dalal, R. C., and Bridge, B. J. (1996), Aggregation and organic matter storage in sub-humid and semi-arid soils. In *Structure and Organic Matter Storage in Agricultural Soils* (M. R. Carter and B. A. Stewart, Eds.), Lewis Publishers, Boca Raton, FL, pp. 263–307.

Escadafal, R., Belgith, A., and Ben Moussa, A. (1994), Indices spectraux pour la télédétéction de la dégradation des milieux naturels en Tunisie aride. In *Proc. 6th Int. Symp. on Physical Measurements and Signatures in Remote Sensing*, 17–24 January 1994, Val d'Isere, France, ESA, Paris, pp. 253–259.

Geiger, F. (1970), Die Aridität in Südostspanien—Ursachen und Auswirkungen im Landschaftswandel. *Stuttgarter Geographische Studien*, 77. Geogr. Inst.: Stuttgart, 173 pp.

Hill, J. (1993), High precision land cover mapping and inventory with multi-temporal earth observation satellite data, The Ardèche experiment. EUR 15271 EN, Office for Official Publications of the European Communities: Luxembourg.

Hill, J., and Sturm, B. (1991), Radiometric correction of multitemporal Thematic Mapper data for use in agricultural landcover classification and vegetation monitoring. *Int. J. Remote Sens.* 12(7):1471–1491.

Hill, J., Mégier, J., and Mehl, W. (1995a), Land degradation, soil erosion and desertification monitoring in Mediterranean ecosystems. *Remote Sens. Rev.* 12:107–130.

Hill, J., Mehl, W., and Radeloff, V. (1995b), Improved forest mapping by combining corrections of atmospheric and topographic effects. In *Sensors and Environmental Applications of Remote Sensing* (J. Askne, Ed.), Proc. 14th EARSeL Symposium, Göteborg, Sweden, 6–8 June 1994, A.A. Balkema, Rotterdam, Brookfield, pp. 143–151.

Hunt, G. R. (1977), Spectral signatures of particulate minerals in the visible and near-infrared. *Geophysics* 42:501–513.

Hunt, G. R., and Salisbury, J. W. (1971), Visible and near-infrared spectra of minerals and rocks, II. Carbonates. *Mod. Geol.* 2:23–30.

Imeson, A.C. (1995), The physical, chemical and biological degradation of the soil. In *Desertification in a European Context: Physical and Socio-economic Aspects* (R. Fantechi, D. Peter, P. Balabanis, and J. L. Rubio, Eds.), Office for Official Publications of the European Communities, Luxembourg, pp. 153–168.

Imeson, A. C., Pérez-Trejo, F., and Cammeraat, L. H. (1996), The response of landscape units to desertification. In *Mediter-*

ranean Desertification and Land Use (C. J. Brandt and J. B. Thornes, Eds.), Wiley, Chichester, pp. 447–469.

Kononova, M. M. (1961), *Soil Organic Matter. Its Role in Soil Formation and Soil Fertility*, Pergamon, London, pp. 47–110.

Krishnan, P., Alexander, D. J., Butler, B. J., and Hummel, J. W. (1980), Reflectance technique for predicting soil organic matter. *Soil Sci. Soc. Am.* 44:1282–1285.

Lacaze, B., Caselles, V., Coll, C., Hill, J., Hoff, C., de Jong, S., Mehl, W., Negendank, J. F. W., Riezebos, H., Rubio, E., Sommer, S., Teixeira Filho, J., and Valor, E. (1996), *Integrated Approaches to Desertification Mapping and Monitoring in the Mediterranean Basin. Final Report of the DeMon-1 Project* (J. Hill, Ed), EUR 16448 EN, Office for Official Publications of the European Communities: Luxembourg.

Leger, R. G., Millette, G. J. F., and Chomchan, S. (1979), The effects of organic matter, iron oxides and moisture on the colour of two agricultural soils of Quebec. *Can. J. Soil Sci.* 59:191–202.

Lynch, J. M., and Bragg, E. (1985), Microorganisms and soil aggregate stability. *Adv. Soil Sci.* 2:133–171.

Nielsen, A. A. (1998), Linear mixture models and partial unmixing in multi- and hyperspectral image data. In *Proceedings of the 1st EARSeL Workshop on Imaging Spectrometry* (M. Schaepman, D. Schläpfer, and K. Itten, Eds.), RSL, University of Zurich, Switzerland, 6–8 October 1998, EARSeL: Paris, pp. 165–172.

Oades, J. M., and Waters, A. G. (1991), Aggregate hierarchy in soils. *Aust. J. Soil Res.* 29:815–828.

Page, N. R. (1974), Estimation of organic matter in Atlantic coastal plain soils with a colour difference meter. *Agron. J.* 66:652–653.

Pickup, G., and Chewings, V. H. (1988), Forecasting patterns of erosion in arid land forms from Landsat MSS data. *Int. J. Remote Sens.* 9:69–84.

Proyecto Lucdeme (1988), *Mapa de Suelos Escala 1:100.000, Lorca-953*, Ministerio de Agricultura, Pesca y Alimentation (MdAPA), Murcia.

Royer, A., Charbonneau, L., and Teillet, P. M. (1988), Interannual Landsat-MSS reflectance variations in an urbanized temperate zone. *Remote Sens. Environ.* 24:423–446.

Schulze, D. G., Nagel, J. L., van Scoyoc, E., Henderson, T. L., and Baumgardner, M. F. (1993), Significance of organic matter in determining soil colours. In *Soil Colour* (J. M. Bingham and E. J. Ciolkosz, Eds.), Madison, Wisconsin, SSSA Special Publication 31, pp. 71–90.

Shields, J. A., Paul, E. A., Arnaud, S., and Head, W. K. (1968), Spectrophotometric measurement of soil colour and its relationship to moisture and organic matter. *Can. J. Soil Sci.* 48:271–280.

Stoner, E. R., and Baumgardner, M. F. (1981), Characteristic variations in reflectance of surface soils. *Soil Sci. Soc. Am. J.* 45:1161–1165.

Tanré, D., Deroo, C., Duhaut, P., Herman, M., Morcrette, J. J., Perbos, J., and Deschamps, P. Y. (1990), Description of a computer code to simulate the signal in the solar spectrum: the 5S code. *Int. J. Remote Sens.* 11(4):659–668.

Thome, K. J., Gellman, D. I., Parada, R. J., Biggar, S. F., Slater, P. N., and Moran, M. S. (1993), In-flight radiometric calibration of Landsat-5 Thematic Mapper, from 1984 to present. In *Recent Advances in Sensors, Radiometric Calibration and Processing of Remotely Sensed Data* (P. Chavez and R. Schowengerdt, Eds.), SPIE Proceedings Vol. 1938, SPIE, Bellingham WA, pp. 126–130.

Thome, K. J., Markham, B., Barker, J., and Biggar, S. F. (1997), Radiometric calibration of Landsat. *Photogramm. Eng. Remote Sens.* 63:853–858.

Tisdall, J. M. (1996), Formation of soil aggregates and accumulation of soil organic matter. In *Structure and Organic Matter Storage in Agricultural Soils* (M. R. Carter and B. A. Stewart, Eds.), Lewis Publishers, Boca Raton, FL, pp. 57–96.

Tisdall, J. M., and Oades, J. M. (1982), Organic matter and water-stable aggregates in soil. *J. Soil Sci.* 33:141–163.

Volk, B. G., and Loeppert, H. (1982), Soil organic matter. In *Handbook of Soils and Climate in Agriculture* (V. J. Kilmer and A. A. Hanson, Eds.), CRC Press, Boca Raton, FL, pp. 211–268.